Cranfield nr. 24

TECHNISCHE UNIVERSITEIT DELFT
LUCHTVAART- EN RUIMTEVAARTTECHNIEK
BIBLIOTHEEK
Kluyverweg 1 - 2629 HS DELFT

Cranfield Institute of Technology

Offshore Engineering Group

12 DEC. 1977

TECHNISCHE HOGESCHOOL DELFT
LUCHTVAART- EN RUIMTEVAARTTECHNIEK
BIBLIOTHEEK
Kluyverweg 1 - DELFT

THE DYNAMIC RESPONSE OF A DOUBLE ARTICULATED OFFSHORE LOADING STRUCTURE TO NON-COLLINEAR WAVES AND CURRENT

R.K. Jain
and
C.L. Kirk

ASME 1977 Summer Applied Mechanics/Bioengineering/Fluids Engineering Conference, Yale University, New Haven Connecticut, U.S.A., June 1977.

THE DYNAMIC RESPONSE OF A DOUBLE ARTICULATED OFFSHORE LOADING STRUCTURE TO NON-COLLINEAR WAVES AND CURRENT

R.K. Jain

C.L. Kirk

Offshore Engineering Group
Cranfield Institute of Technology,
Cranfield, Bedford, England.

The dynamic response of a double articulated structure to non-collinear Airey waves and a steady current is studied for various waves and varying current directions. The governing equations of motion are derived by Lagrange's method where wave and current forces are computed by a modified form of Morison's equation which takes account of relative motion of water particles with respect to the oscillating structure. The resulting equations are highly non-linear and are solved numerically by using a block integration method. The computed results predict complex whirling oscillations of the structure to non-collinear waves and current.

Introduction

With increasing offshore activity and its extension to deeper and rougher waters, such as encountered in the North Sea, there is a growing need of cost effective, reliable, light weight and easy to install offshore structures for initial development, subsequent production and loading purposes. An increasing use of mobile systems for storage and loading of oil into attendant tankers is to be expected in coming years. This is particularly true for oil fields that have a limited production capability or are too remote from the refining or terminal points to warrant the laying of a pipeline. Mobile loading structures are also used as an interim measure during pipeline laying for large fields and, in case of pipeline failure, as a back-up system. Typical mobile loading and storage systems are: single articulated tower, double articulated tower or single point mooring system (S.P.M.), tension leg buoy, etc. In spite of their importance, relatively little research work has been reported, particularly for articulated systems. The present authors[1] have investigated the dynamic response of a single articulated tower to waves and current. Dyer[2] studied the response of a double articulated loading structure to waves only.

This paper is concerned with the development of a mathematical model of a two-pin articulated offshore loading structure subjected to non-collinear ocean waves and a steady current. The structure is composed of two parts. The lower part or the riser is a long, narrow cylinder attached to the sea bed through a universal joint. The upper part consists of a buoyant cylinder or buoy attached to the riser through another universal joint. The buoy has a main flotation chamber of comparatively large diameter with a small diameter cylinder at the top. On top of the buoy lies a deck and other attachments. The resultant buoyancy force of the system can be changed by varying the ballast loads in the riser and the buoy.

The structure is designed so that the upper flotation chamber remains submerged. The advantage of this type of structure, apart from light weight, lies in the fact that the universal joints permit the S.P.M. to move with the water particles rather than resist their motion. The system has four degrees of freedom and its equations of motion have been derived by Lagrange's method where the wave and current forces are evaluated by using a modified form of Morison's equation to take account of relative motion of fluid particles with respect to the structure. The resulting equations are highly non-linear and analytical solutions are not possible. Therefore, numerical solutions based on a block integration technique [4] are carried out for various cases of waves and current. An equivalent set of linear equations is also unobtainable for the general case, so that random analysis of the problem by spectral methods is not feasible.

Double articulated structures are designed to allow maximum rotations of 17° and 37° from the vertical of the riser and buoy sections respectively. This is the case under extreme conditions due to the combined action of wind, waves and current forces. It is found that the structure investigated in this paper appears to be quite stable under the extreme case of 100 year design wave which has a period of 17 sec. and height of 30 metres. For non-collinear waves and current, a complex whirling motion is predicted.

In the present investigation, the tanker is not attached to the S.P.M. The tanker will alter the response but this will depend on the size and manner in which it is moored to the S.P.M. The present analysis, however, gives very useful information about the estimated deflections of the structure, under severe environmental forces, which is necessary to determine the survival conditions. In moderate sea states, it gives the estimated motion of the system relative to an approaching tanker for mooring purposes.

Description of Problem

A schematic of the double articulated offshore loading structure or a single point mooring system (SPM) is shown in Figure 1. It consists of a riser of uniform diameter D_1, length ℓ_1 and a universal joint at the bottom end O_1 which is fixed to a rigid block at the sea bed. The upper part of the structure consists of a buoyant cylinder or buoy attached to the riser through a second universal joint at O_2.

The buoy has a main chamber of diameter $D_2 > D_1$ and length ℓ_2. The upper part of the buoy is also a cylinder of diameter $D_3 < D_2$ and length ℓ_3. On top of this part lies a deck and other attachments. The total buoyancy force can be changed by varying the ballast loads in the lower and upper parts of the structure which is designed so that the main flotation chamber remains below the S.W.L. The universal joints at 0_1 and 0_2 allow the S.P.M. to move with the water particle motion rather than to resist it.

The instantaneous position of the structure during motion is depicted in Figure 2, where the fixed orthogonal reference axes X, Y and Z are so chosen that XZ plane is parallel to the sea bed with origin at 0_1. Another set of orthogonal coordinates x, y and z is chosen parallel to X, Y and Z system with a moving origin at 0_2. The instantaneous position of the structure is completely determined by four angles θ_1, θ_2, ψ_1, ψ_2. As shown in Figure 2, θ_1 and ψ_1 determine the position of the riser whereas θ_2 and ψ_2 determine the position of upper part of the structure. The angle θ_1 is the meridianal angle which the axis $0_1 0_2$ makes with Y-axis and ψ_1 is the circumferential angle between the planes $Y0_1 0_2$ and $Y0_1 Z$. The angles θ_2, ψ_2 are similarly defined for the upper part with reference to the coordinate system x, y, z.

The system is subjected to the simultaneous action of linear waves propagating in the X-direction and a steady current of velocity V(Y) which may vary with water depth and whose direction makes an angle α with the X-axis. In the absence of waves, the system acquires a static equilibrium position due to current drag force described by angular coordinates $(\theta_{10}, \frac{\pi}{2} - \alpha)$ and $(\theta_{20}, \frac{\pi}{2} - \alpha)$.Under the combined action of waves and current, the structure will perform oscillatory motion either in or out of the XZ-plane depending on whether the waves and current are collinear or non-collinear.

Static Equilibrium due to Current

In the present investigation the current is assumed to be steady and its velocity to vary with the water depth in a linear manner. The current vector $\overline{V}(Y)$ makes an angle α with the X-axis and has its magnitude given by the expression

$$V(Y) = V_c(V_{co} + \beta Y/d), \qquad (1)$$

where V_c is a constant and gives the current speed at the still water level (SWL), and

$$V_{co} = V_o/V_c,$$

$$\beta = 1 - V_{co}$$

V_o is the current speed at the sea bed; d is the water depth from SWL.

Under the action of current, the structure is displaced to a static equilibrium position determined by two pairs of angular coordinates $(\theta_{10}, \frac{\pi}{2} - \alpha)$ and $(\theta_{20}, \frac{\pi}{2} - \alpha)$. The meridional angles θ_{10} and θ_{20} are given by the following two equations of equilibrium

$$-\left[M^{(1)}h_g^{(1)}+M_{B\ell}h_{B\ell}/2-M_f^{(1)}\ell_1/2+M_p(\ell_1+h_2/2)+(M^{(2)}+M^{(3)}-M_f^{(2)}-M_f^{(3)}+M_T)(\ell_1+h_2)\right]g\sin\theta_{10}$$
$$= \frac{2C_D}{\pi} V_c^2 \left[M_f^{(1)}\gamma_1\frac{\ell_1}{D_1} + \left(1+\frac{h_2}{\ell_1}\right)\left\{M_f^{(2)}\gamma_2\frac{\ell_1}{D_2} + M_f^{(3)}\gamma_3\frac{\ell_1}{D_3}\frac{\ell_3'}{\ell_3}\right\}\right]\cos\theta_{10} \tag{2a}$$

and

$$-\left[M^{(2)}h_g^{(2)}+M^{(3)}(\ell_2+h_g^{(3)})+M_T(\ell_2+\ell_3)-M_f^{(2)}\ell_2/2-M_f^{(3)}(\ell_2+\ell_3'/2)\right]g\sin\theta_{20}$$
$$= \frac{2C_D}{\pi} V_c^2 \left[M_f^{(2)}\gamma_4\frac{\ell_2}{D_2} +M_f^{(3)}\gamma_5 \frac{\ell_3'^2}{\ell_3 D_3}\right]\cos\theta_{20} \tag{2b}$$

To obtain equations (2), the drag forces in the vertical position of the structure have been considered.

In equations (2a) and (2b) $M^{(i)}$, $i = 1,2,3$, are the structural masses of the riser, the buoy and the top cylindrical portion, respectively; $M_f^{(i)}$, $i = 1,2,3$ are the masses of fluid displaced by these three parts; $h_g^{(i)}$, $i = 1,2,3$ are the respective centres of gravity; M_p is the mass of the pin at O_2 and the disc above it; M_T is deck and swivel mass at the top; $M_{B\ell}$ is mass of ballast in the riser and $h_{B\ell}$ is the height to which the ballast fills it; h_1 is height of pin O_1 from the sea bed and h_2 is height of pin at O_2 ; ℓ_3' is the submerged depth of top cylinder ; C_D is coefficient of drag and $\gamma_1, \gamma_2, \ldots, \gamma_5$ are given by the following expressions:

$$\gamma_1 = V_{co}^2/2 + 2V_{co}\bar{\beta}/3 + \bar{\beta}^2/4,$$

$$\gamma_2 = (V_{co} + \bar{\beta}^2) + (V_{co} + \bar{\beta})\bar{\beta}\,\ell_2/\ell_1 + \bar{\beta}^2/3\;\ell_2^2/\ell_1^2,$$

$$\gamma_3 = \{V_{co} + \bar{\beta}(1 + \ell_2/\ell_1)\}^2 + \{V_{co} + \bar{\beta}(1 + \ell_2/\ell_1)\}\bar{\beta}\ \ell_3'/\ell_1$$

$$+ \bar{\beta}^2/3\ \ell_3'^2/\ell_1^2 ,$$

$$\gamma_4 = (V_{co} + \bar{\beta})^2/2 + 2/3(V_{co} + \bar{\beta})\bar{\beta}\ \ell_2/\ell_1 + \bar{\beta}^2/4\ \ell_2^2/\ell_1^2$$

$$\gamma_5 = \{V_{co} + \bar{\beta}(1 + \ell_2/\ell_1)\}^2/2 + 2/3\{V_{co} + \bar{\beta}(1 + \ell_2/\ell_1)\}\beta\ell_3'/\ell_1$$

$$+ \bar{\beta}^2\ell_3'^2/\ell_1^2,$$

where $\bar{\beta} = \beta\ell_1/d$.

The right hand side terms in equations (2a), (2b) represent the moments of fluid drag acting on the structure. The riser and buoy are assumed to be of uniform diameters and constant thickness so that the centres of gravity lie at the geometrical centres, i.e.

$$h_g^{(i)} = \ell_i/2, \quad i = 1,2,3.$$

Furthermore, for current speeds of practical interest V_c is found to be between 2 to 5 knots for the northern North Sea. For these current speeds the static displacements θ_{10}, θ_{20} will be small so that equations (2a) and (2b) yield simple expressiond for these angles on substituting

$$\sin\theta_{i0} = \theta_{i0}, \quad \cos\theta_{i0} = 1, \quad i = 1,2 .$$

The Dynamic Analysis of Response

The equations of motion of the structure subjected to non-collinear waves and current are derived by the method of Lagrange. It is assumed that the structure oscillates as a rigid body which is justified because the rigid body displacements are much bigger than the elastic deformations of the structure. As such the wave forces are not significantly affected by the elastic vibrations of the structure. Any coupling between the rigid and elastic modes will result in added complexities in the already complex system. However, the bending moments and shear forces can be determined from the knowledge of rigid structural response where a static analysis can be performed by considering the wave forces at any instant. This procedure should yield all the information needed in design.

To derive the equations, the kinetic energy and potential energy are first calculated followed by computation of wave forces.

Kinetic Energy of the Structure

As mentioned in the previous section, the instantaneous position of the structure is completely determined by two pairs of angular coordinates (θ_1, ψ_1), and (θ_2, ψ_2). The position vector of any point distance r_1 from O_1 on the riser is

$$\underset{\sim}{r}^{(1)}(r_1) = r_1\left[C_x^{(1)}, C_y^{(1)}, C_z^{(1)}\right] , \qquad (4)$$

where $C_x^{(1)}$, $C_y^{(1)}$, $C_z^{(1)}$ are direction cosines of the axis O_1O_2;

$$\begin{aligned} C_x^{(1)} &= \sin\theta_1\sin\psi_1 , \\ C_y^{(1)} &= \cos\theta_1 , \\ C_z^{(1)} &= \sin\theta_1\cos\psi_1 . \end{aligned} \qquad (5)$$

Similarly, the position vector of any point on the upper part of the structure is

$$\underset{\sim}{r}^{(2)}(r_2) = \underset{\sim}{r}^{(1)}(\ell_1 + h_2) + r_2\left[C_x^{(2)}, C_y^{(2)}, C_z^{(2)}\right], \qquad (6)$$

where r_2 is the distance from O_2; $C_x^{(2)}$, $C_y^{(2)}$, $C_z^{(2)}$ are direction cosines of the axis O_2O_3:

$$\begin{aligned} C_x^{(2)} &= \sin\theta_2\sin\psi_2 , \\ C_y^{(2)} &= \cos\theta_2 , \\ C_z^{(2)} &= \sin\theta_2\cos\psi_2 . \end{aligned} \qquad (7)$$

The kinetic energy of the structure is then given as

$$T = \frac{1}{2}\Bigg[\int_0^{\ell_1} m_1 \dot{\underset{\sim}{r}}^{(1)}(r_1)\cdot\dot{\underset{\sim}{r}}^{(1)}(r_1)dr_1 + \int_0^{h_{B\ell}} m_{B\ell}\dot{\underset{\sim}{r}}^{(1)}(r_1)\cdot\dot{\underset{\sim}{r}}^{(1)}(r_1)dr_1 + M_p\dot{\underset{\sim}{r}}^{(1)}(\ell_1+\frac{h_2}{2})\cdot\dot{\underset{\sim}{r}}^{(1)}(\ell_1+\frac{h_2}{2})$$

$$+ \int_0^{\ell_2} m_2\dot{\underset{\sim}{r}}^{(2)}(r_2)\cdot\dot{\underset{\sim}{r}}^{(2)}(r_2)dr_2 + \int_{\ell_2}^{L_2} m_3\dot{\underset{\sim}{r}}^{(2)}(r_2)\cdot\dot{\underset{\sim}{r}}^{(2)}(r_2)dr_2$$

$$+ M_T\dot{\underset{\sim}{r}}^{(2)}(L_2)\cdot\dot{\underset{\sim}{r}}^{(2)}(L_2)\Bigg], \qquad (8)$$

where $L_2 = \ell_2+\ell_3$; m_1, m_2, m_3 and $m_{B\ell}$ are mass densities of the riser, the buoy, the cylinder C_3 and of ballast per unit length, respectively. The dots denote differentiation with respect to time.

On substituting from equations (6) and (7) into equation (8), and after integration, we get

$$T = \frac{1}{2}\Big[I_1(\dot\theta_1^2 + \sin^2\theta_1\dot\psi_1^2) + I_2(\dot\theta_2^2 + \sin^2\theta_2\dot\psi_2^2)$$

$$+ 2I_3(k_1\dot\theta_1\dot\theta_2 + k_2\dot\psi_1\dot\psi_2 + k_3\dot\theta_1\dot\psi_2 + k_4\dot\theta_2\dot\psi_2)\Big], \qquad (9)$$

where

$$I_1 = \int_0^{\ell_1} m_1 r_1^2 dr_1 + \int_0^{h_{B\ell}} m_{B\ell} r_1^2 dr_1 + \left\{\int_0^{\ell_2} m_2 dr_2 + \int_{\ell_2}^{L_2} m_3 dr_2 + M_T\right\}(\ell_1+h_2)^2$$

$$+ M_p(\ell_1 + \frac{h_2}{2})^2,$$

$$I_2 = \int_0^{\ell_2} m_2 r_2^2 dr_2 + \int_{\ell_2}^{L_2} m_3 r_2^2 dr_2 + M_T L_2^2, \qquad (10)$$

$$I_3 = \left\{\int_0^{\ell_2} m_2 r_2 dr_2 + \int_{\ell_2}^{L_2} m_3 r_2 dr_2 + M_T L_2\right\}(\ell_1+h_2).$$

As mentioned earlier, the cylinders have uniformly distributed mass, which gives

$$I_1 = \left[\frac{1}{3}(M^{(1)} + M_{B\ell}\frac{h_{B\ell}^2}{\ell_1^2}) + (M^{(2)}+M^{(3)}+M_T)(1+h_2/\ell_1)^2 + M_p(1+\frac{h_2}{2\ell_1})^2\right]\ell_1^2,$$

$$I_2 = \left[\frac{1}{3}M^{(2)}\frac{\ell_2^2}{\ell_1^2} + M^{(3)}(\frac{L_2^2}{\ell_1^2} + \frac{L_2}{\ell_1}\frac{\ell_2}{\ell_1} + \frac{\ell_2^2}{\ell_1^2}) + M_T\frac{L_2^2}{\ell_1^2}\right]\ell_1^2, \qquad (11)$$

$$I_3 = \left[\frac{1}{2}\left\{M^{(2)}\frac{\ell_2}{\ell_1} + M^{(3)}(\frac{L_2}{\ell_1} + \frac{\ell_2}{\ell_1})\right\} + M_T\frac{L_2}{\ell_1}\right](1 + \frac{h_2}{\ell_1})\,\ell_1^2,$$

and

$$\begin{aligned} k_1 &= \cos\theta_1\cos\theta_2\cos(\psi_1-\psi_2) + \sin\theta_1\sin\theta_2 , \\ k_2 &= \sin\theta_1\sin\theta_2\cos(\psi_1-\psi_2) , \\ k_3 &= \cos\theta_1\sin\theta_2\sin(\psi_1-\psi_2) , \\ k_4 &= -\sin\theta_1\cos\theta_2\sin(\psi_1-\psi_2) . \end{aligned} \qquad (12)$$

The Potential Energy of the Structure

The displacement of the structure will cause the weight and buoyancy forces to do work due to rotations θ_1 and θ_2. The change in potential energy of the riser is found to be

$$V_L = -\{M^{(1)}h_g^{(1)}+M_{B\ell}h_{B\ell}/2 + M_p(\ell_1+h_2/2)- M_f^{(1)}h_B^{(1)}\}(1-\cos\theta_1)g.$$

The change in potential energy of the buoy and the deck mass is found to be

$$\begin{aligned} V_U = &-\{M^{(2)}+M^{(3)}+M_T-M_f^{(2)}-M_f^{(3)}\}(\ell_1+h_2)(1-\cos\theta_1)g \\ &-\{M^{(2)}h_g^{(2)}+M^{(3)}h_g^{(3)}+M_TL_2-M_f^{(2)}\ell_2/2-M_f^{(3)}(\ell_2+\ell_3'/2)\}(1-\cos\theta_2)g. \end{aligned}$$

The total potential energy of the structure is thus

$$V = -M_t^{(1)}(1-\cos\theta_1)g-M_t^{(2)}(1-\cos\theta_2)g, \qquad (13)$$

where

$$\begin{aligned} M_t^{(1)} = &M^{(1)}h_g^{(1)}+M_{B\ell}h_{B\ell}/2-M_f^{(1)}h_B^{(1)}+M_p(\ell_1+h_2/2) \\ &+(\ell_1+h_2)\{M^{(2)}+M^{(3)}+M_T-M_f^{(2)}-M_f^{(3)}\} , \end{aligned} \qquad (14a)$$

$$M_t^{(2)} = M^{(2)}h_g^{(2)}+M^{(3)}h_g^{(3)}+M_TL_2-M_f^{(2)}\frac{\ell_2}{2} - M_f^{(3)}(\ell_2+\ell_3'/2). \qquad (14b)$$

Equations of Motion

The equations of motion of the structure can now be obtained by applying Lagrange's equation

$$\frac{d}{dt}\left[\frac{\partial T}{\partial \dot{q}_i}\right] + \frac{\partial}{\partial q_i}(V-T) = M_q^{(i)}, \quad q = \theta, \psi, \quad i = 1, 2.$$

The four equations thus obtained are

$$I_1\ddot{\theta}_1+I_3(k_1\ddot{\theta}_2+k_3\ddot{\psi}_2)+I_3K_1-I_1\sin\theta_1\cos\theta_1\dot{\psi}_1{}^2-M_t^{(1)}g\sin\theta_1 = M_\theta^{(1)}, \quad (15a)$$

$$I_2\ddot{\theta}_2+I_3(k_1\ddot{\theta}_1+k_4\ddot{\psi}_1)+I_3K_2-I_2\sin\theta_2\cos\theta_2\dot{\psi}_2{}^2-M_t^{(2)}g\sin\theta_2 = M_\theta^{(2)}, \quad (15b)$$

$$I_1\sin^2\theta_1\ddot{\psi}_1+I_3(k_2\ddot{\psi}_2+k_4\ddot{\theta}_2)+I_3K_3+2I_1\sin\theta_1\cos\theta_1\dot{\theta}_1\dot{\psi}_1 = M_\psi^{(1)}, \quad (15c)$$

$$I_2\sin^2\theta_2\ddot{\psi}_2+I_3(k_2\ddot{\psi}_1+k_3\ddot{\theta}_1)+I_3K_4+2I_2\sin\theta_2\cos\theta_2\dot{\theta}_2\dot{\psi}_2 = M_\psi^{(2)}, \quad (15d)$$

where

$$K_1 = -\cos\theta_1\sin\theta_2\cos(\psi_1-\psi_2)(\dot{\theta}_2{}^2+\dot{\psi}_2{}^2)+ \sin\theta_1\cos\theta_2\dot{\theta}_2{}^2 + 2\cos\theta_1\cos\theta_2\sin(\psi_1-\psi_2)\dot{\theta}_2\dot{\psi}_2, \quad (16a)$$

$$K_2 = -\sin\theta_1\cos\theta_2\cos(\psi_1-\psi_2)(\dot{\theta}_1{}^2+\dot{\psi}_1{}^2)+\cos\theta_1\sin\theta_2\dot{\theta}_1{}^2 - 2\sin\theta_1\cos\theta_2\sin(\psi_1-\psi_2)\dot{\theta}_1\dot{\psi}_1 , \quad (16b)$$

$$K_3 = \sin\theta_1\sin\theta_2\sin(\psi_1-\psi_2)(\dot{\theta}_2{}^2+\dot{\psi}_2{}^2)+2\sin\theta_1\cos\theta_2\cos(\psi_1-\psi_2)\dot{\theta}_2\dot{\psi}_2, \quad (16c)$$

$$K_4 = -\sin\theta_1\sin\theta_2\sin(\psi_1-\psi_2)(\dot{\theta}_1{}^2+\dot{\psi}_1{}^2)+2\cos\theta_1\sin\theta_2\cos(\psi_1-\psi_2)\dot{\theta}_1\dot{\psi}_1, \quad (16d)$$

and $M_\theta^{(1)}$, $M_\theta^{(2)}$, $M_\psi^{(1)}$ and $M_\psi^{(2)}$ are the moments of fluid forces on the system. The moments $M_\theta^{(1)}$ and $M_\theta^{(2)}$ are moments about O_1X' and O_2X', respectively; $M_\psi^{(1)}$ and $M_\psi^{(2)}$ are the moments about O_1Y and O_2y respectively. These moments are derived in the following sections.

Wave Forces and their Moments

The wave forces on the structure are derived by applying Morison's equation [3] modified to incorporate the relative velocities and accelerations of fluid particles with respect to the structural members. The diameters of the component cylinders are small compared to wave lengths of practical interest thus the non-linear drag forces cannot be neglected in the Morison's equation.

Assuming a potential flow, the velocity components of fluid particles can be derived from the potential function

$$\phi(X,Y,t) = \frac{gH}{2\omega}\,\frac{\cosh k(Y+h_1)}{\cosh kd}\,\sin\{k(X-ct)+\chi\} , \quad (17)$$

where H is wave height; ω , k, c and χ denote wave frequency, wave number, wave velocity and wave phase, respectively; d is the water depth from the mean water level. The wave number, wave frequency and wave velocity are related to the wave length L and wave period T by the following relations

$$k = 2\pi/L ,$$
$$\omega = 2\pi/T ,$$
$$c = \frac{gT}{2\pi} \tanh\left(\frac{2\pi d}{L}\right) ,$$
where
$$T = \left(\frac{2\pi L}{g}\right)/\tanh\left(\frac{2\pi d}{L}\right) .$$

Drag Forces

The water particle velocity vector is obtained from the potential function, equation (17). It is

$$\dot{\underset{\sim}{u}}(X,Y,t) = [u_X, u_Y, 0]^T , \quad (18)$$

where

$$u_X = \frac{\pi H}{T} \frac{\cosh k(Y+h_1)}{\sinh(kd)} \cos\{k(X-ct) + \chi\},$$

$$u_Y = \frac{\pi H}{T} \frac{\sinh k(Y+h_1)}{\sinh(kd)} \sin\{k(X-ct) + \chi\}.$$

The current direction makes an angle α with the X-axis, so that

$$\underset{\sim}{V}(Y) = [V_X, 0, V_Z]^T,$$

where
$$V_X(Y) = |\underset{\sim}{V}| \cos\alpha,$$
$$V_Z(Y) = |\underset{\sim}{V}| \sin\alpha .$$

It is assumed that the fluid velocity vectors due to waves and current can be added, in which case the resultant particle velocity is given by

$$\underset{\sim}{u}_r(X,Y,t) = [u_X+V_X, u_Y, V_Z]^T.$$

Since the forces on the structure are caused mainly by the fluid motion normal to its cylindrical components, the components of resultant fluid velocity vector normal to the riser and the buoy parts are evaluated. These are given respectively as

$$\underset{\sim}{u}_n^{(1)}(X,Y,t) = A^{(1)}\underset{\sim}{u}_r(X,Y,t), \quad (19a)$$

and

$$\underset{\sim}{u}_n^{(2)}(\bar{x},\bar{y},t) = A^{(2)}\underset{\sim}{u}_r(\bar{x},\bar{y},t). \quad (19b)$$

where $(X, Y) = r_1[C_x^{(1)}, C_y^{(1)}]$,

$$(\bar{x}, \bar{y}) = (\ell_1+h_2)[C_x^{(1)}, C_y^{(1)}] + r_2[C_x^{(2)}, C_y^{(2)}] ,$$

and $A^{(i)}$, $i = 1,2$ are symmetric matrices of order 3 whose elements are

$$A_{11}^{(i)} = 1 - \{C_x^{(i)}\}^2 ,$$
$$A_{12}^{(i)} = -C_x^{(i)}C_y^{(i)} ,$$
$$A_{13}^{(i)} = -C_x^{(i)}C_z^{(i)} ,$$
$$A_{22}^{(i)} = 1 - \{C_y^{(i)}\}^2 ,$$
$$A_{23}^{(i)} = -C_y^{(i)} C_z^{(i)} ,$$
$$A_{33}^{(i)} = 1 - \{C_z^{(i)}\}^2 ,$$

where direction cosines $C_x^{(i)}$, $C_y^{(i)}$, $C_z^{(i)}$ are given in equations (5) and (7).

The velocities of the elements of the structure distance r_1 from O_1 and r_2 from O_2 are obtained from equations (4) and (6). These are

$$\underset{\sim}{v}^{(1)}(r_1) = r_1[V_1^{(1)}, V_2^{(1)}, V_3^{(1)}]^T ,$$
$$\underset{\sim}{v}^{(2)}(r_2) = v_1^{(1)}(\ell_1+h_2) + r_2[V_1^{(2)}, V_2^{(2)}, V_3^{(2)}]^T ,$$

where

$$V_1^{(i)} = \cos\theta_i\sin\psi_i\dot{\theta}_i + \sin\theta_i\cos\psi_i\dot{\psi}_i ,$$

$$V_2^{(i)} = -\sin\theta_i\ \dot{\theta}_i ,$$

$$V_3^{(i)} = \cos\theta_i\cos\psi_i\dot{\theta}_i - \sin\theta_i\sin\psi_i\dot{\psi}_i .$$

Thus the relative normal velocities of the fluid particles are found to be

$$\underset{\sim}{V}_R^{(1)}(X, Y, t) = \underset{\sim}{u}_n^{(1)}(X, Y, t) - \underset{\sim}{v}^{(1)}(r_1) , \qquad (20a)$$

$$\underset{\sim}{V}_R^{(2)}(\bar{x}, \bar{y}, t) = \underset{\sim}{u}_n^{(2)}(\bar{x}, \bar{y}, t) - \underset{\sim}{v}^{(2)}(r_2),\ 0 \le r_2 \le L_2' \qquad (20b)$$

where $L_2' = \ell_2 + \ell_3'$.

The non-linear drag forces per unit length of the structure are, respectively

$$\underset{\sim}{F}_D^{(1)}(r_1) = \frac{\rho}{2} C_D \, D_1 \underset{\sim}{V}_R^{(1)} \, |\underset{\sim}{V}_R^{(1)}| \; , \tag{21a}$$

$$\underset{\sim}{F}_D^{(2)}(r_2) = \frac{\rho}{2} C_D \, D_2 \underset{\sim}{V}_R^{(2)} \, |\underset{\sim}{V}_R^{(2)}| \; , \; 0 \leq r_2 \leq \ell_2 \tag{21b}$$

$$\underset{\sim}{F}_D^{(3)}(r_2) = \frac{\rho}{2} C_D \, D_3 \underset{\sim}{V}_R^{(2)} \, |\underset{\sim}{V}_R^{(2)}| \; , \; \ell_2 < r_2 \leq L_2 \tag{21c}$$

where ρ is mass density of water; C_D is the drag coefficient.

Forces due to Fluid Inertia

The acceleration of the fluid particles is given by the vector

$$\dot{\underset{\sim}{u}}(X, Y, t) = [\dot{u}_X, \dot{u}_Y, 0]^T,$$

where

$$\dot{u}_X(X,Y,t) = \frac{2\pi^2 H}{T^2} \frac{\cosh\{k(Y+h_1)\}}{\sinh \; (kd)} \sin\{k(X-ct) + \chi\},$$

$$\dot{u}_Y(X,Y,t) = \frac{-2\pi^2 H}{T^2} \frac{\sinh\{k(Y+h_1)\}}{\sinh(kd)} \cos\{k(X-ct) + \chi\}.$$

The components of fluid acceleration normal to the structural members are computed in the manner of equations (19). Thus the normal components of fluid inertia force per unit length of the structure along the three parts are given as

$$\underset{\sim}{F}_I^{(1)}(r_1) = \rho\pi \frac{D_1^2}{4} C_m \, A^{(1)} \dot{\underset{\sim}{u}} \quad , \tag{22a}$$

$$\underset{\sim}{F}_I^{(2)}(r_2) = \rho\pi \frac{D_2^2}{4} C_m \, A^{(2)} \dot{\underset{\sim}{u}} \quad , \quad 0 \leq r_2 \leq \ell_2 \tag{22b}$$

$$\underset{\sim}{F}_I^{(3)}(r_2) = \rho\pi \frac{D_3^2}{4} C_m \, A^{(2)} \dot{\underset{\sim}{u}} \quad , \quad \ell_2 < r \leq L_2' \tag{22c}$$

where C_m is the coefficient of fluid inertia.

Forces due to Fluid Added Mass

The acceleration vectors of the elements of the structure whose distances from O_1 and O_2 are r_1 and r_2, respectively, are

$$\underset{\sim}{a}^{(1)}(r_1) = r_1[a_1^{(1)}, a_2^{(1)}, a_3^{(1)}]^T,$$

and $\underset{\sim}{a}^{(2)}(r_2) = \underset{\sim}{a}^{(1)}(\ell_1+h_2) + r_2[a_1^{(2)}, a_2^{(2)}, a_3^{(2)}]^T,$

where

$$a_1^{(i)} = -(\dot{\theta}_i^2 + \dot{\psi}_i^2)\sin\theta_i\sin\psi_i + 2\dot{\theta}_i\dot{\psi}_i\cos\theta_i\cos\psi_i + \ddot{\theta}_i\cos\theta_i\sin\psi_i + \ddot{\psi}_i\sin\theta_i\cos\psi_i,$$

$$a_2^{(i)} = -\theta_i^2\cos\theta_i - \ddot{\theta}_i\sin\theta_i ,$$

$$a_3^{(i)} = -(\dot{\theta}_i^2+\dot{\psi}_i^2)\sin\Theta_i\cos\Psi_i - 2\dot{\Theta}_i\dot{\Psi}_i\cos\Theta_i\sin\Psi_i + \ddot{\Theta}_i\cos\Theta_i\cos\Psi_i - \ddot{\Psi}_i\sin\Theta_i\sin\Psi_i .$$

The normal forces per unit length of the structure due to fluid added mass are given as

$$\underset{\sim}{F}_A^{(1)}(r_1) = -\rho\pi\frac{D_1^2}{4}C_m^* \underset{\sim}{a}^{(1)}(r_1), \tag{23a}$$

$$\underset{\sim}{F}_A^{(2)}(r_2) = -\rho\pi\frac{D_2^2}{4}C_m^* \underset{\sim}{a}^{(2)}(r_2), \quad 0 \le r_2 \le \ell_2 \tag{23b}$$

$$\underset{\sim}{F}_A^{(3)}(r_2) = -\rho\pi\frac{D}{4}C_m^* \underset{\sim}{a}^{(2)}(r_2), \quad \ell_2 < r_2 \le L_2' , \tag{23c}$$

where C_m^* is the added mass coefficient.

Substituting into the Morison's equation,

$$\underset{\sim}{F}_n = \underset{\sim}{F}_D + \underset{\sim}{F}_I - \underset{\sim}{F}_A,$$

from equations (21)-(23), the total normal forces per unit length of the structural members are obtained as

$$\underset{\sim}{F}_n^{(i)} = \underset{\sim}{F}_D^{(i)} + \underset{\sim}{F}_I^{(i)} - \underset{\sim}{F}_A^{(i)} , \qquad i = 1,2,3 \tag{24}$$

<u>Moments of Wave Forces</u>

The moments of wave forces, equation (24), about O_1X' and O_2x' are given as

$$M_\theta^{(1)} = \int_0^{\ell_1} r_1 W_1^{(1)} dr_1 + (\ell_1+h_2)\left[\int_0^{\ell_2} W_1^{(2)} dr_2 + \int_{\ell_2}^{\ell_2+\ell_3'} W_1^{(3)} dr_2\right], \tag{25a}$$

and

$$M_\theta^{(2)} = \int_0^{\ell_2} r_2 W_2^{(2)} dr_2 + \int_{\ell_2}^{\ell_2+\ell_3'} r_2 W_2^{(3)} dr_2 , \tag{25b}$$

where

$$W_j^{(i)} = F_{nx}^{(i)}\cos\theta_j\sin\psi_j + F_{nz}^{(i)}\cos\theta_j\cos\psi_j - F_{ny}^{(i)}\sin\theta_j \quad ,$$

and $F_{nx}^{(i)}$, $F_{ny}^{(i)}$, $F_{nz}^{(i)}$ are the components of $F_n^{(i)}$ in X, Y and Z direction respectively.

The moments about O_1Y and O_2y are found to be

$$M_\psi^{(1)} = \int_0^{\ell_1} r_1 V_1^{(1)} dr_1 + (\ell_1+h_2)\left[\int_0^{\ell_2} V_1^{(2)} dr_2 + \int_{\ell_2}^{\ell_2+\ell_3'} V_1^{(3)} dr_2\right], \quad (25c)$$

$$M_\psi^{(2)} = \int_0^{\ell_2} r_2 V_2^{(2)} dr_2 + \int_{\ell_2}^{\ell_2+\ell_3'} r_2 V_2^{(3)} dr_2, \quad (25d)$$

where

$$V_j^{(i)} = F_{nx}^{(i)}\sin\theta_j\cos\psi_j - F_{nz}^{(i)}\sin\theta_j\sin\psi_j \ .$$

<u>Final Form of Equations of Motion</u>

The inertial forces due to added mass $\underset{\sim}{F}_A^{(i)}$ can be divided into two parts - one which is dependent on structural accelerations $\ddot\theta_1, \ddot\theta_2, \ddot\psi_1$ and $\ddot\psi_2$, and the second part which is a function of structural velocities. Substituting from equations (25) into equations (15) and transposing the terms containing second order derivatives to the left hand side, the final equations of motion are then obtained in the form

$$A_{11}\theta_1'' + A_{12}\theta_2'' + A_{14}\psi_2'' = f_1(\tau,\theta_1,\theta_2,\psi_1,\psi_2,\theta_1',\theta_2',\psi_1',\psi_2'), \quad (26a)$$

$$A_{12}\theta_1'' + A_{22}\theta_2'' + A_{23}\psi_1'' = f_2(\tau,\theta_1,\theta_2,\psi_1,\psi_2,\theta_1',\theta_2',\psi_1',\psi_2'), \quad (26b)$$

$$A_{23}\theta_2'' + A_{33}\psi_1'' + A_{34}\psi_2'' = f_3(\tau,\theta_1,\theta_2,\psi_1,\psi_2,\theta_1',\theta_2',\psi_1',\psi_2'), \quad (26c)$$

$$A_{14}\theta_1'' + A_{34}\psi_1'' + A_{44}\psi_2'' = f_4(\tau,\theta_1,\theta_2,\psi_1,\psi_2,\theta_1',\theta_2',\psi_1',\psi_2'), \quad (26d)$$

in which $\tau = t/T$ is the non-dimensional time parameter and dashes denote derivatives with respect to τ;

$$A_{11} = \bar{I}_1 + C_m^* b_{11} \ ,$$

$$A_{12} = (\bar{I}_3 + C_m^* b_{12})k_1 \ ,$$

$$A_{14} = (\bar{I}_3 + C_m^* b_{12})k_3 \ ,$$

$$A_{22} = \bar{I}_2 + C_m^* b_{22} \quad ,$$

$$A_{23} = (\bar{I}_3 + C_m^* b_{12})k_4 \ ,$$

$$A_{33} = (\bar{I}_1 + C_m^* b_{11})\sin^2\theta_1 \quad ,$$

$$A_{34} = (\bar{I}_3 + C_m^* b_{12})k_2 \quad ,$$

$$A_{44} = (\bar{I}_2 + C_m^* b_{22})\sin^2\theta_2 \ ;$$

$$(\bar{I}_1, \bar{I}_2, \bar{I}_3) = (I_1, I_2, I_3)/(M_f^{(1)} \ell_1^2);$$

$$b_{11} = \frac{1}{3} + \left\{\frac{D_2^2}{D_1^2}\frac{\ell_2}{\ell_1} + \frac{D_3^2}{D_1^2}\left(\frac{L_2'}{\ell_1} - \frac{\ell_2}{\ell_1}\right)\right\}\left(1 + \frac{h_2}{\ell_1}\right)^2,$$

$$b_{12} = \frac{1}{2}\left\{\frac{D_2^2}{D_1^2}\frac{\ell_2^2}{\ell_1^2} + \frac{D_3^2}{D_1^2}\left(\frac{L_2'^2}{\ell_1^2} - \frac{\ell_2^2}{\ell_1^2}\right)\right\}\left(1 + \frac{h_2}{\ell_1}\right),$$

$$b_{22} = \frac{1}{3}\left\{\frac{D_2^2}{D_1^2}\frac{\ell_2^3}{\ell_1^3} + \frac{D_3^2}{D_1^2}\left(\frac{L_2'^3}{\ell_1^3} - \frac{\ell_2^3}{\ell_1^3}\right)\right\};$$

$$f_1(\tau, \dots) = \frac{T^2}{M_f^{(1)} \ell_1^2} m_\theta^{(1)} - \bar{I}_3 \bar{K}_1 + \bar{I}_1 \sin\theta_1 \cos\theta_1 \psi_1'^2 + \frac{M_t^{(1)}}{M_f^{(1)} \ell_1} \frac{gT^2}{\ell_1} \sin\theta_1,$$

$$f_2(\tau, \dots) = \frac{T^2}{M_f^{(1)} \ell_1^2} m_\theta^{(2)} - \bar{I}_3 K_2 + \bar{I}_2 \sin\theta_2 \cos\theta_2 \psi_2'^2 + \frac{M_t^{(2)}}{M_f^{(1)} \ell_1} \frac{gT^2}{\ell_1} \sin\theta_2,$$

$$f_3(\tau, \dots) = \frac{T^2}{M_f^{(1)} \ell_1^2} m_\psi^{(1)} - \bar{I}_3 \bar{K}_3 - 2\bar{I}_1 \sin\theta_1 \cos\theta_1 \theta_1' \psi_1',$$

$$f_4(\tau, \dots) = \frac{T^2}{M_f^{(1)} \ell_1^2} m_\psi^{(2)} - \bar{I}_3 \bar{K}_4 - 2\bar{I}_2 \sin\theta_2 \cos\theta_2 \theta_2' \psi_2',$$

where $m_\theta^{(1)}$, $m_\theta^{(2)}$, $m_\psi^{(1)}$ and $m_\psi^{(2)}$ are the same as given in equations (25) but without θ_1'', θ_2'', ψ_1'' and ψ_2'' terms; $\bar{K}_1$, $\bar{K}_2$, $\bar{K}_3$ and $\bar{K}_4$ are the same as given in equations (16) but real time derivatives are replaced by non-dimensional time derivatives.

The initial conditions of the problem are

$$\theta_1(0) = \theta_{10},\ \theta_2(0) = \theta_{20},\ \theta_1'(0) = 0,\ \theta_2'(0) = 0,$$

and

$$\psi_1(0) = \frac{\pi}{2} - \alpha,\ \psi_2(0) = \frac{\pi}{2} - \alpha,\ \psi_1'(0) = 0,\ \psi_2'(0) = 0.$$

Equations (26) are coupled, highly non-linear equations with time dependent coefficients and as such a closed form solution is not possible. Furthermore, these equations cannot be linearised in either least square sense or otherwise due to presence of angles ψ_1 and ψ_2. Thus random analysis by spectral methods is not possible. Again due to the complex form of these equations, analytical investigation into stability of the system is not feasible. In fact singularities will occur in the solution when either θ_1 or θ_2 is of the order of zero. This is due to the form of coefficients A_{33} and A_{44}.

Results and Discussion

As was pointed out in the previous section, the analytical solution of equations (26) is not possible due to their non-linear nature. If the forces due to current were to be ignored, the system would reduce to one of two degrees of freedom which can then be linearised if a further assumption of small displacements is made. A spectral approach would then enable the random response of the structure to be obtained which is the object of a separate study by the authors. In the present case, however, numerical solutions of the system are obtained by a 4th order block integration method using two block points [4]. By this method, displacements and velocities at two points $t_1 = t_0 + \Delta t$ and $t_2 = t_0 + 2\Delta t$, where Δt is the time step, are simultaneously computed if initial conditions in terms of displacements and velocities are prescribed at $t = t_0$. The accelerations at t_2 are also obtained as a bi-product. The local truncation errors at t_2 are of the order of $(\Delta t)^5$ and at t_1 they are of the order of $(\Delta t)^4$. However, the lower local accuracy at t_1 does not affect subsequent computations since only values at t_2 are required for the next set of block points. Most results given in this paper were computed with $(\Delta t/T) = 0.02$ and 0.01. The system is quite stable but singularities can occur if either θ_1 or θ_2 tend to zero. This happens in the general case only due to the form of the coefficients as pointed out in the last section.

If the current direction is not orthogonal to the direction of wave propagation, the wave length is modified due to the increase or decrease in wave velocity since the wave period remains constant. The modified wave length L' is given by

$$L' = L(1 + V_x/c) ,$$

or

$$L' = L\left\{1 + V_x\sqrt{\frac{2}{gL\tanh(kd)}}\right\}.$$

A maximum of 4.5 per cent change in wave length occurred in the present study.

The natural undamped frequencies of the S.P.M. are obtained from equations (15 a,b) by assuming linear undamped motions with small displacements in XY-plane. Ignoring non-linear terms and writing $\psi_1 = \psi_2 = \frac{\pi}{2}$, $\dot{\psi}_i = \ddot{\psi}_i = 0$, $\sin\theta_i = \theta_i$, $\cos\theta_i = 1$, for i = 1, 2 and $k_1 = 1$, the following equations of free oscillations are obtained.

$$c_{11}\ddot{\theta}_1 + c_{12}\ddot{\theta}_2 - c_{13}\frac{g}{\ell_1}\theta_1 = 0,$$

$$c_{12}\ddot{\theta}_1 + c_{22}\ddot{\theta}_2 - c_{23}\frac{g}{\ell_1}\theta_2 = 0,$$

where

$$c_{11} = \bar{I}_1 + C_m^* b_{11},$$

$$c_{12} = \bar{I}_3 + C_m^* b_{12},$$

$$c_{13} = M_t^{(1)}/M_f^{(1)}\ell_1,$$

$$c_{22} = \bar{I}_2 + C_m^* b_{22},$$

$$c_{23} = M_t^{(2)}/M_f^{(1)}\ell_1.$$

The two natural sway frequencies are given by

$$\omega^2_{n_{1,2}} = \frac{g}{2\ell_1}\left\{(c_{13}c_{22} + c_{23}c_{11}) \pm U^{\frac{1}{2}}\right\}/(c_{12}^2 - c_{11}c_{22}) \quad ,$$

where

$$U = (c_{13}c_{22} - c_{23}c_{11})^2 + 4c_{13}c_{23}c_{12}^2 .$$

The structural data used in the computations is representative of a typical double articulated structure designed for use in water depths of around 160 metres. The data is as follows;

$D_1/\ell_1 = D_3/\ell_1 = 0.025$; $D_2/\ell_1 = 0.04$;

$\ell_2/\ell_1 = 0.4$; $\ell_3/\ell_1 = 0.2$; $d/\ell_1 = 1.60$;

$h_{B\ell}/\ell_1 = 0.4$; $h_1/\ell_1 = 0.06$; $h_2/\ell_1 = 0.02$;

$M^{(1)}/M_f^{(1)} = 0.3040$; $M^{(2)}/M_f^{(1)} = 0.1169$; $M^{(3)}/M_f^{(1)} = 0.0609$;

$M_{B\ell}/M_f^{(1)} = 0.36$; $M_T/M_f^{(1)} = 0.0012$; $M_p/M_f^{(1)} = 0.038$.

The following values of current and wave data were used

$$C_D = 0.6, 1.0 \; ; \; C_m = 2.0 \; ; \; C_m^* = 1.0 \; ;$$

$$\bar{V}_c = [V_c^2/\ell_1 g]^{\frac{1}{2}} = 0.035 \; ; \; V_o = 0.0 \; ;$$

$$L/\ell_1 = 4.0, 1.0 \; ; \quad H/\ell_1 = 0.3, 0.1 \; .$$

The length of the riser of a typical S.P.M. is about 100 metres. For ℓ_1 = 100 metres, the above data represents a structure for which the diameters of the riser, the buoyant chamber and the top cylinder are 2.5 m, 4.0 m and 2.5 m, respectively. The corresponding water depth is 160 metres. For this structure, the natural sway frequencies, from equation (27), are found to be 0.229 and 0.703 rad/sec with time periods of 27.45 and 8.94 sec. respectively. The combination L/ℓ_1 = 4.0 and H/ℓ_1 = 0.3 represents a wave of period 16 sec and height of 30 metres. This case henceforth will be referred to as the 'design wave' case.

The response histories were computed for trains of three waves. The wave and current forces were computed at the displaced position of the structure in all cases. For comparison, however, response histories in some cases were also computed with wave forces evaluated at the undisplaced position. These are shown by broken lines in Figures 3-8.

The results in Figures 3-8 illustrate the effects of varying values of C_D and the wave parameters. The superimposition of current on waves modifies the response characteristics. It is observed that it is not merely the superimposition of a static response due to current on the oscillatory response due to waves. The modification of wave length due to current changes the wave forces on the structure also. The superimposition of current is expected to modify values of C_D which will also change with the varying direction of the current. But no data is at present available which could be used. Therefore the values of C_D were not changed in the computations. In fact for a greater accuracy, values of C_D which depend on water depth, wave frequency, Keulegn-Carpenter number and surface roughness should be used [5], but information in respect of structures subjected to real ocean waves is not readily available. After all the sea is highly random in its behaviour so the effort at obtaining more precise values in a deterministic case may not be worth the time involved in such a work.

Figures 3-5, describe the response of structure to collinear waves and current. The sway response X/ℓ_1 of the point O_2 are plotted in Figures 3a-5a, whereas displacements X/ℓ_1 of the top from the Y-axis are plotted in Figures 3b-5b. In these diagrams, the broken lines depict the response histories when the wave and current forces on the structure are calculated in the undisturbed position. The solid lines depict the response obtained for the cases where the forces are computed in the instantaneous position of the structure. The response histories corresponding to non-collinear waves and current are plotted in Figures 6-8.

Referring to the response curves, it is observed that the structure oscillates almost at the wave frequency but with a small phase lag. The effect of the non-collinear current is to perturb the sway motion in the direction of current which results in the three dimensional complex whirling oscillations of the structure as shown in Figures 6-8. As expected the non-collinear current flow causes a reduction in the maximum swaying displacement which is a minimum for orthogonal waves and current. In the present investigation, maximum sway angles $\theta_1 = 14^0$ and $\theta_2 = 18^0$ were obtained for the case of collinear waves and current both moving in the same direction.

Since the natural sway periods of the S.P.M. are 27.45 and 8.94 seconds respectively, it can be seen that in a fully developed sea state the response can occur in both modes as the wave spectrum will contain significant energy at these periods.

REFERENCES

1. C.L. Kirk and R.K. Jain, "Response of Articulated Towers to Waves and Current", Proceedings of the 1977 Offshore Technology Conference, Houston, Texas, 1977, pp.545-552.

2. R.C. Dyer, "Wave Induced Motions of Articulated Mooring Towers", MSc Thesis, Cranfield Institute of Technology, England, 1976.

3. S.R. Morison et al, "The Force Exerted by Surface Waves on Piles", Petroleum Transactions, AIME, Vol.189, 1950, pp.149-157.

4. J.D. Lambert, Computational Methods in Ordinary Differential Equations John Wiley and Sons, London, 1973, p.156.

5. T. Sarpkaya, "Vortex Shedding and Resistance in Harmonic Flow about Smooth and Rough Circular Cylinders", Proceedings of International Conference on the Behaviour of Offshore Structures, Norwegian Institute of Technology, Trondheim, Norway, Vol,1, 1976, pp.220-235.

Acknowledgements

This work was supported by S.R.C. Grants B/RG/3464 and GR/A/04590.

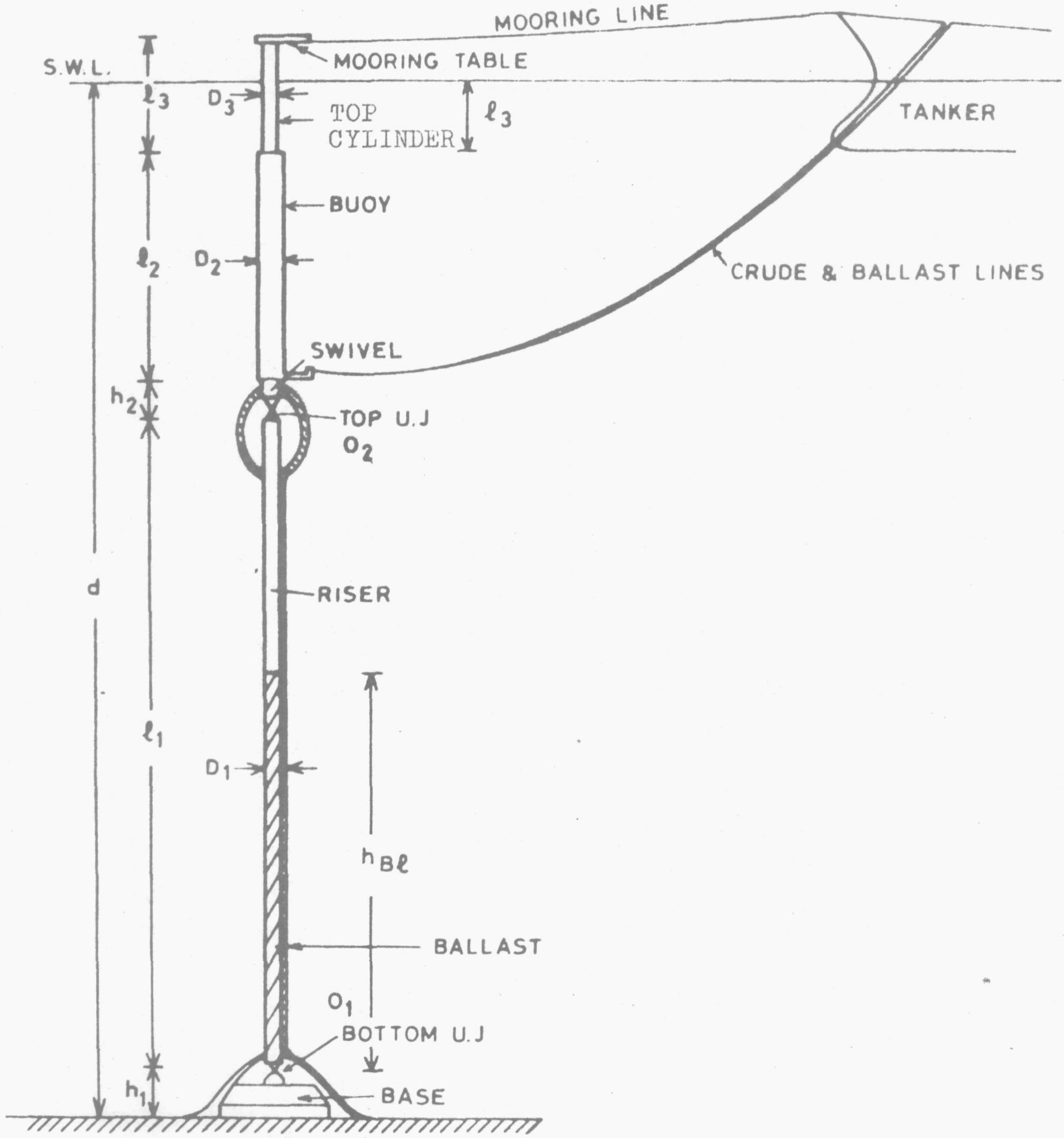

Fig. 1

Schematic of a double articulated offshore loading structure

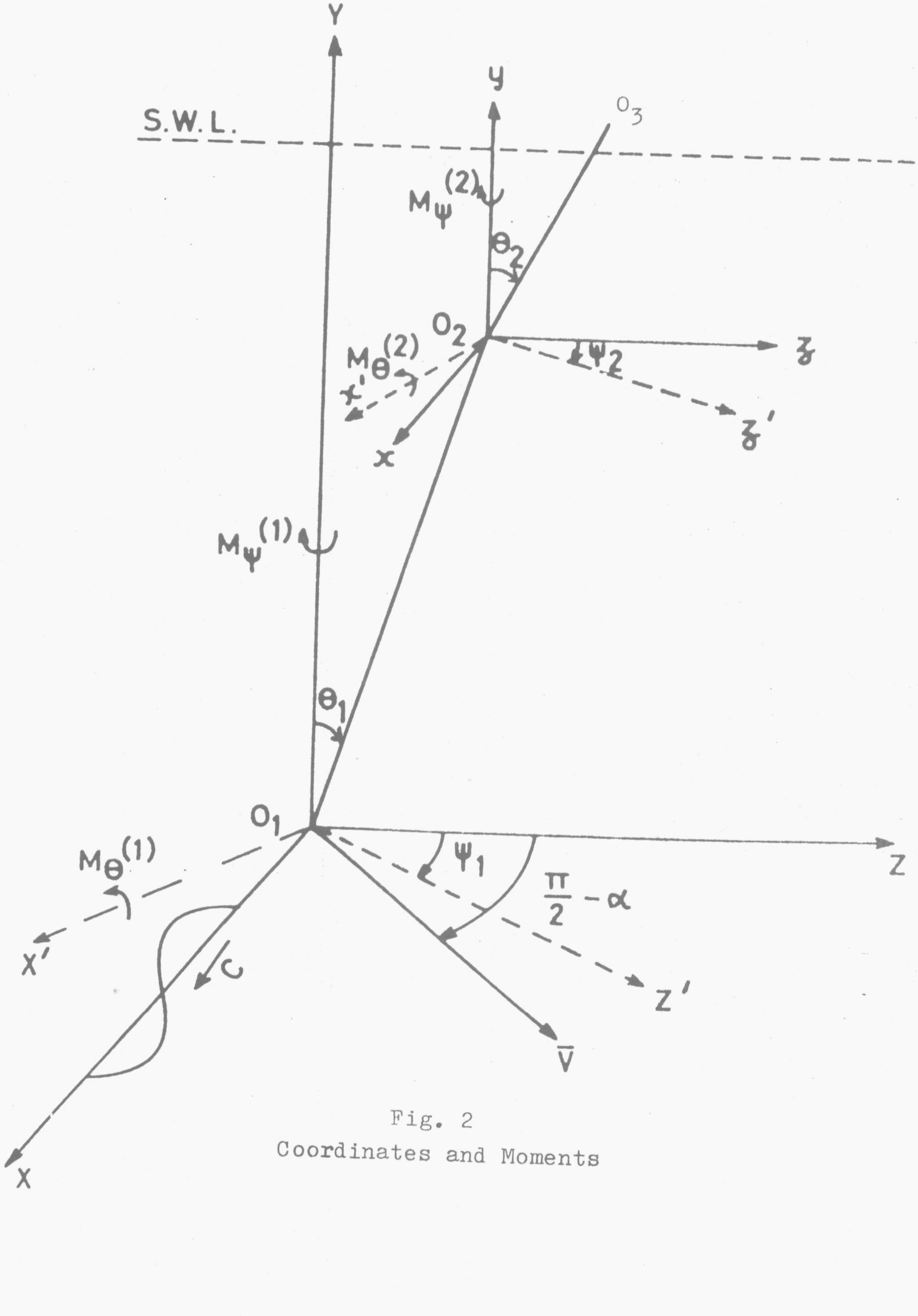

Fig. 2
Coordinates and Moments

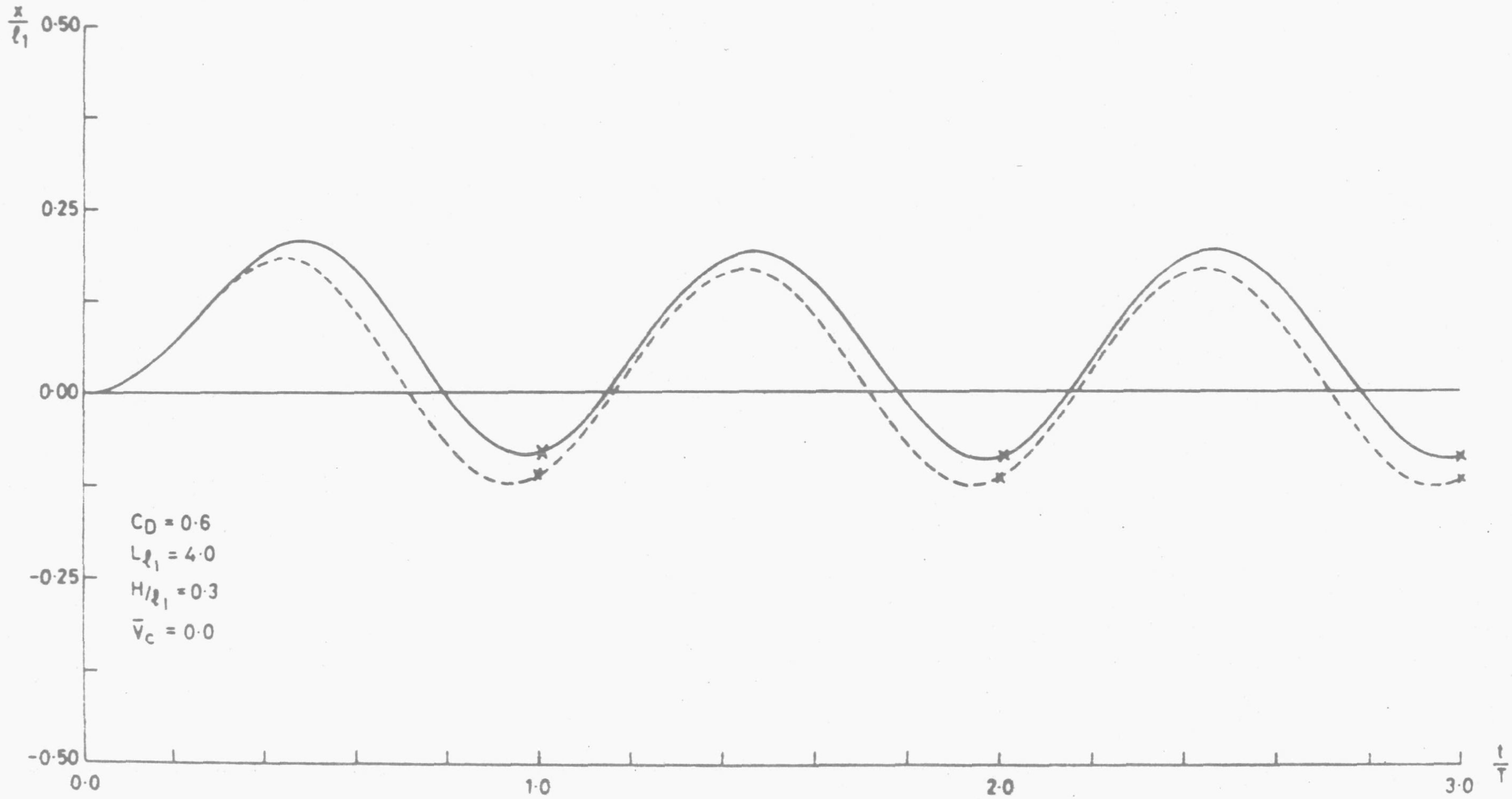

Fig. 3a

Sway response to waves only - Point C_2

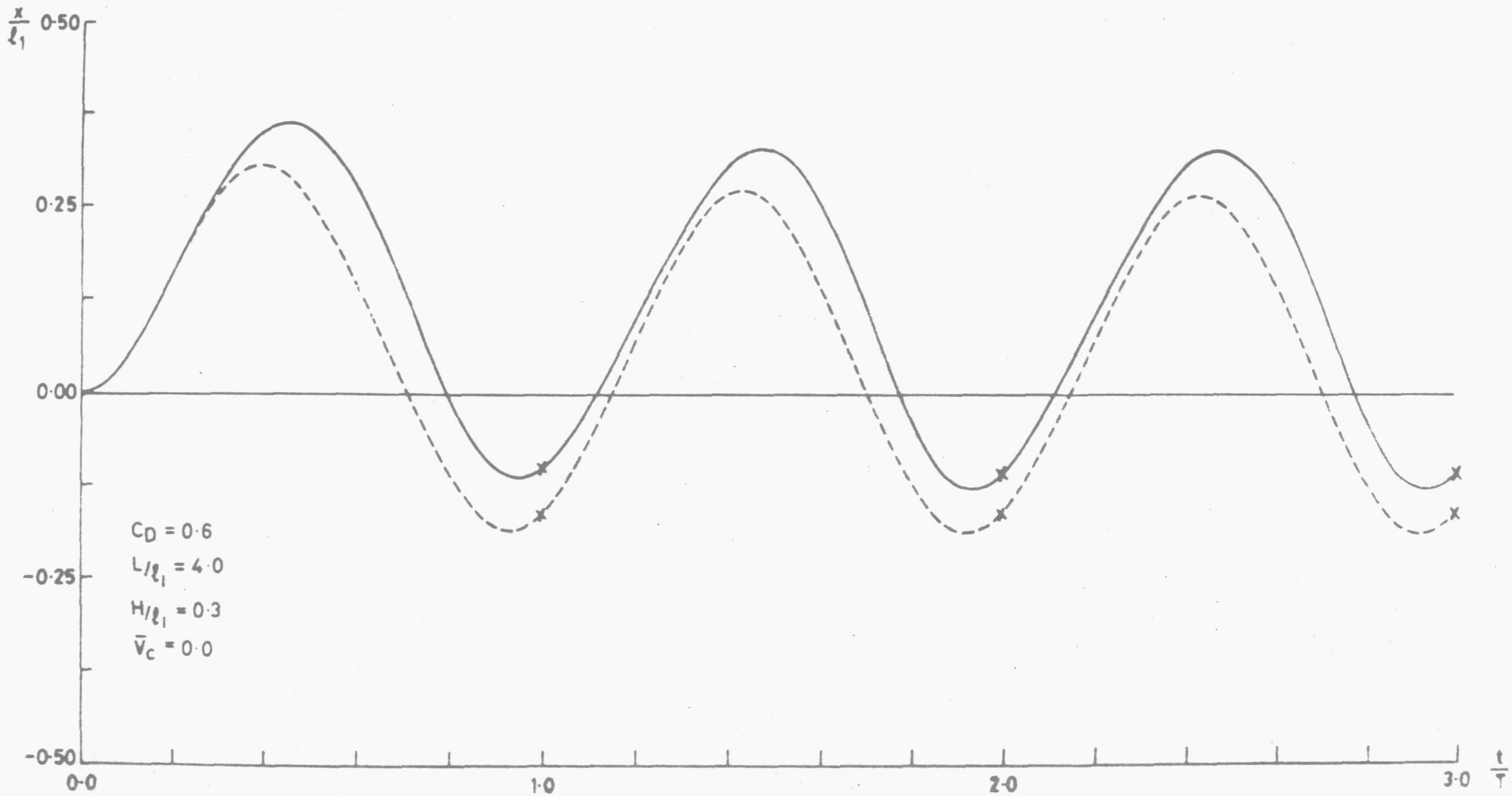

Fig. 3b

Sway response to waves only - Top

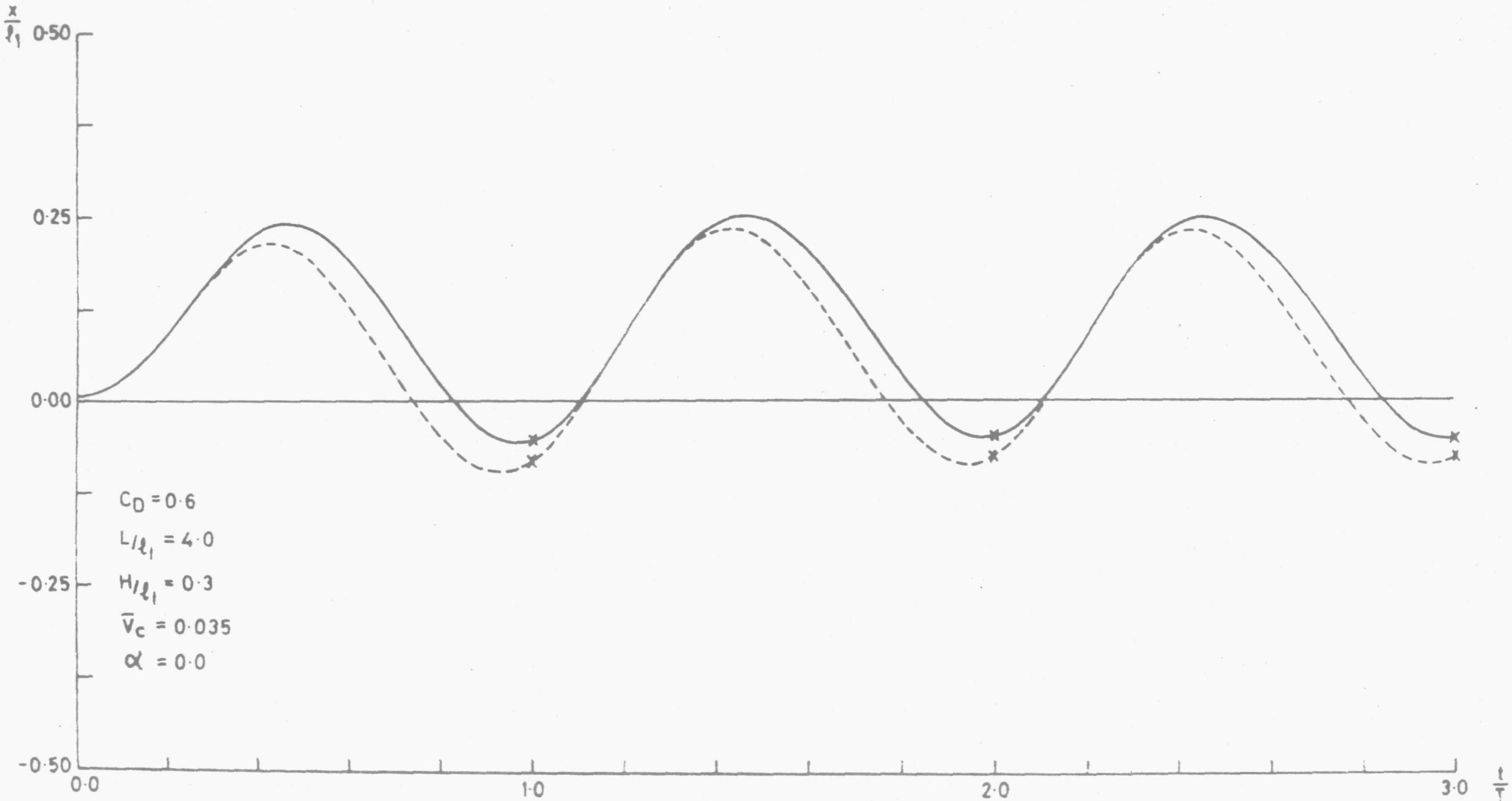

Fig. 4a

Sway response to waves and following current - Point O_2

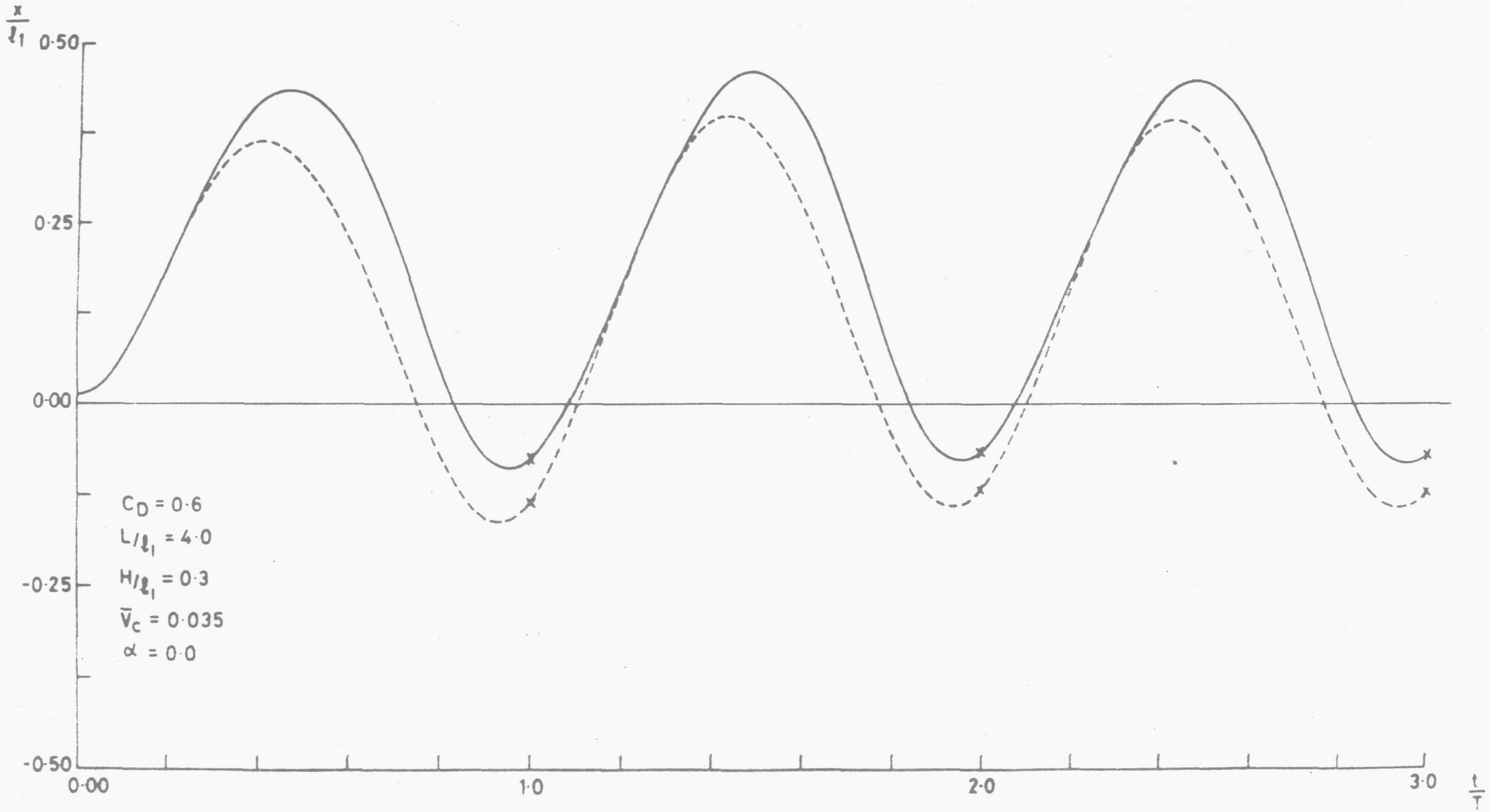

Fig. 4b

Sway response to waves and following current - Top

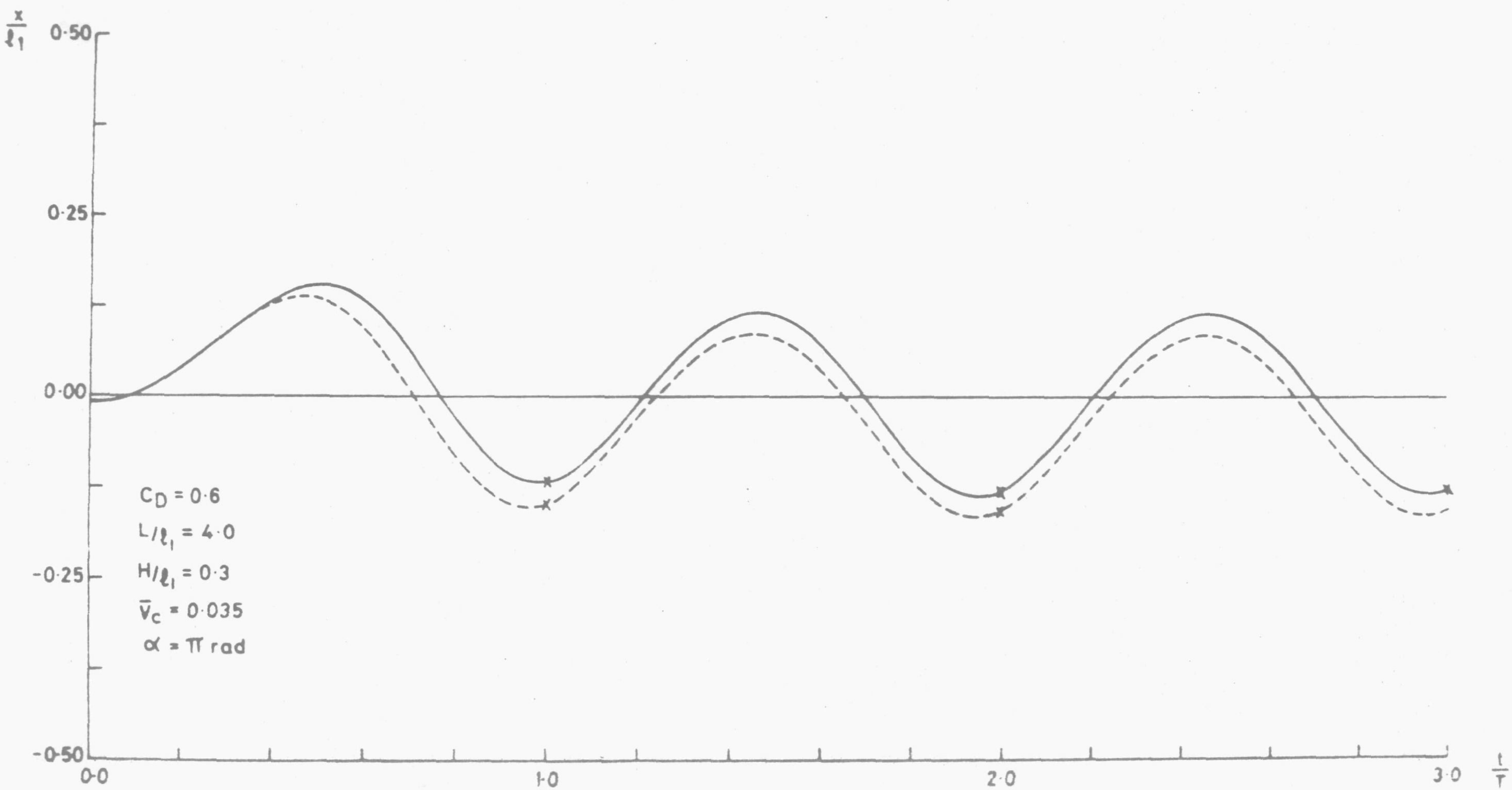

Fig. 5a

Sway response to waves and opposing current - Point O_2

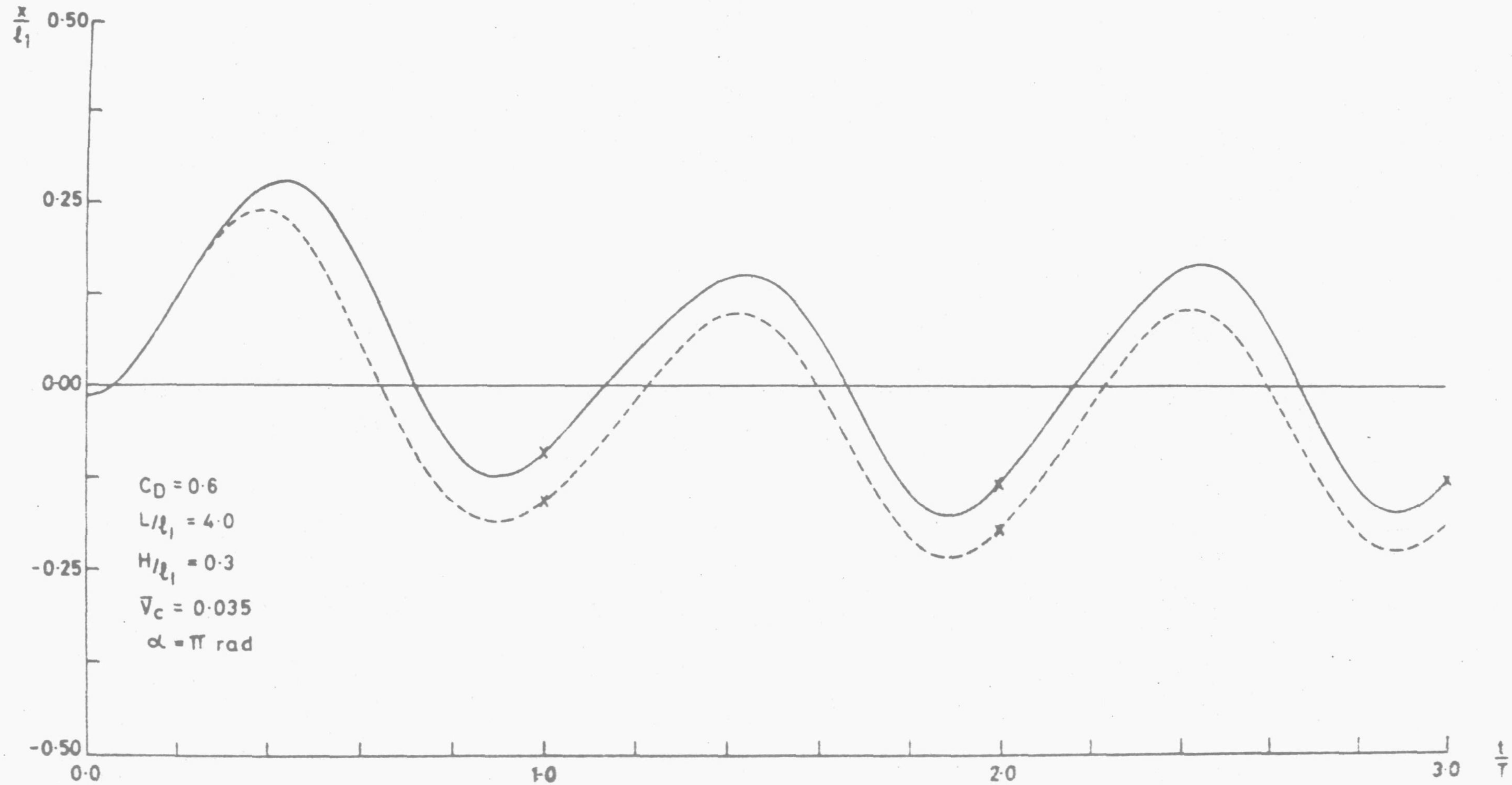

Fig. 5b

Sway response to waves and opposing current - Top

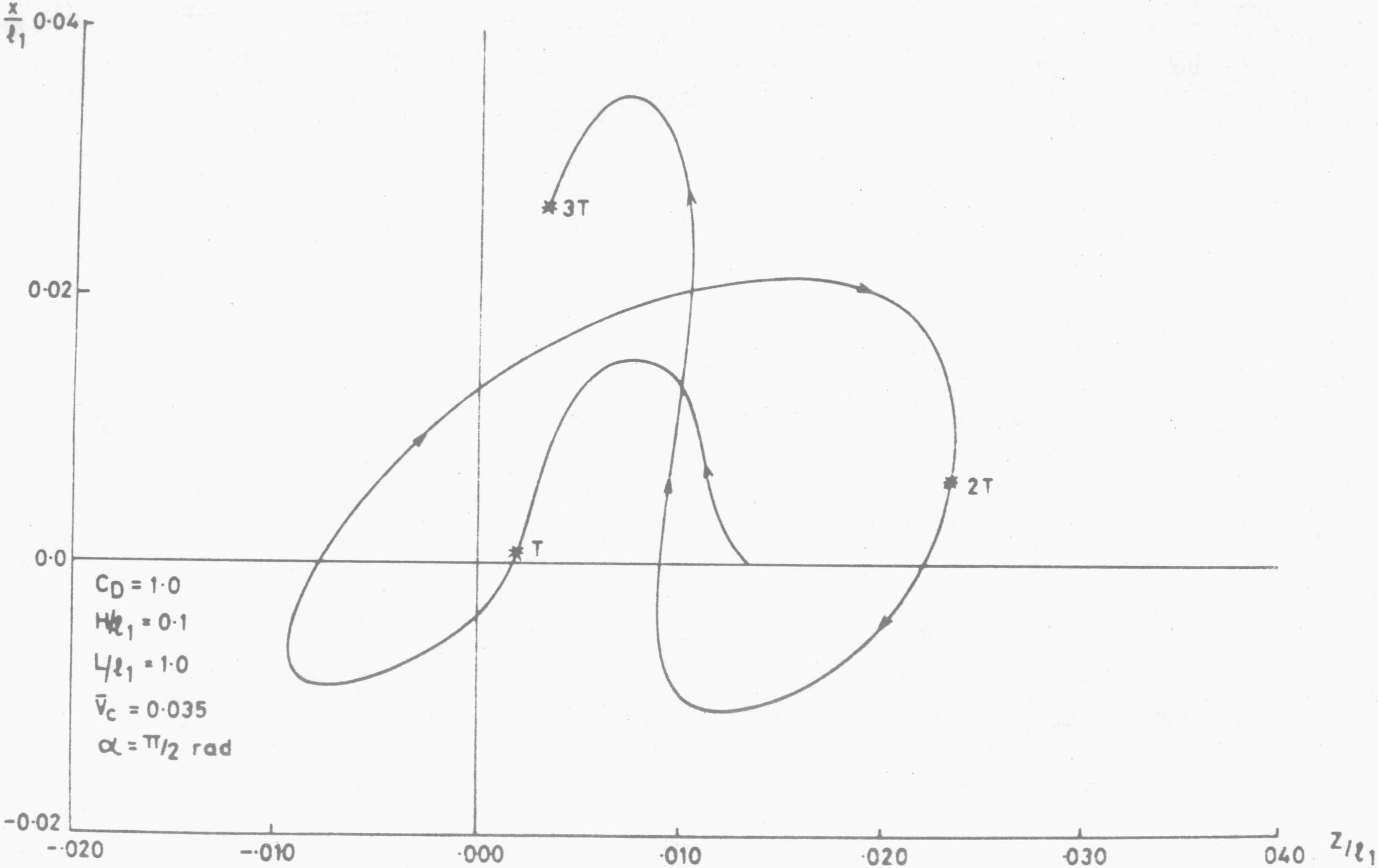

Fig. 6a

Response to orthogonal waves and current - Point O_2

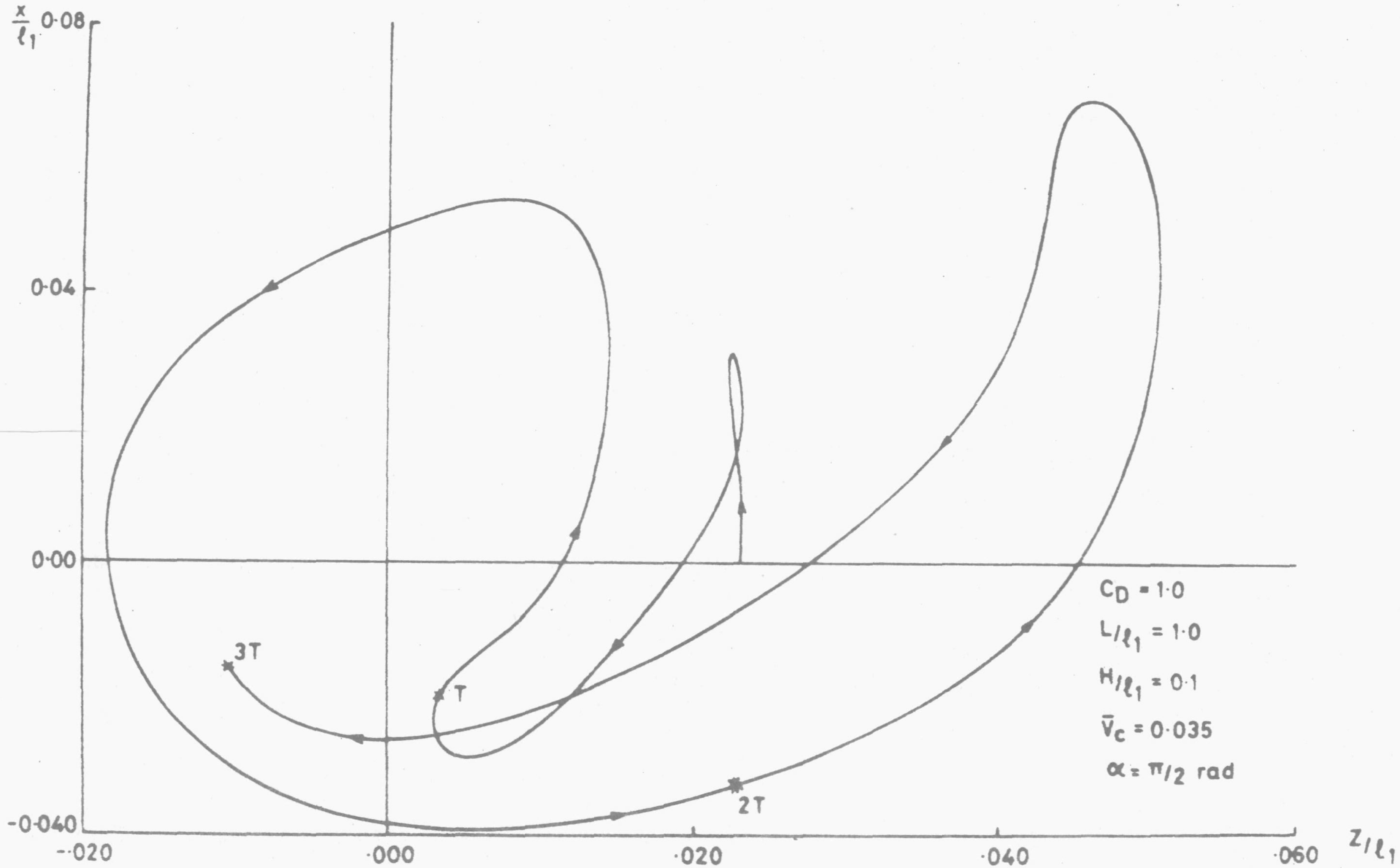

Fig. 6b

Response to orthogonal waves and current - Top

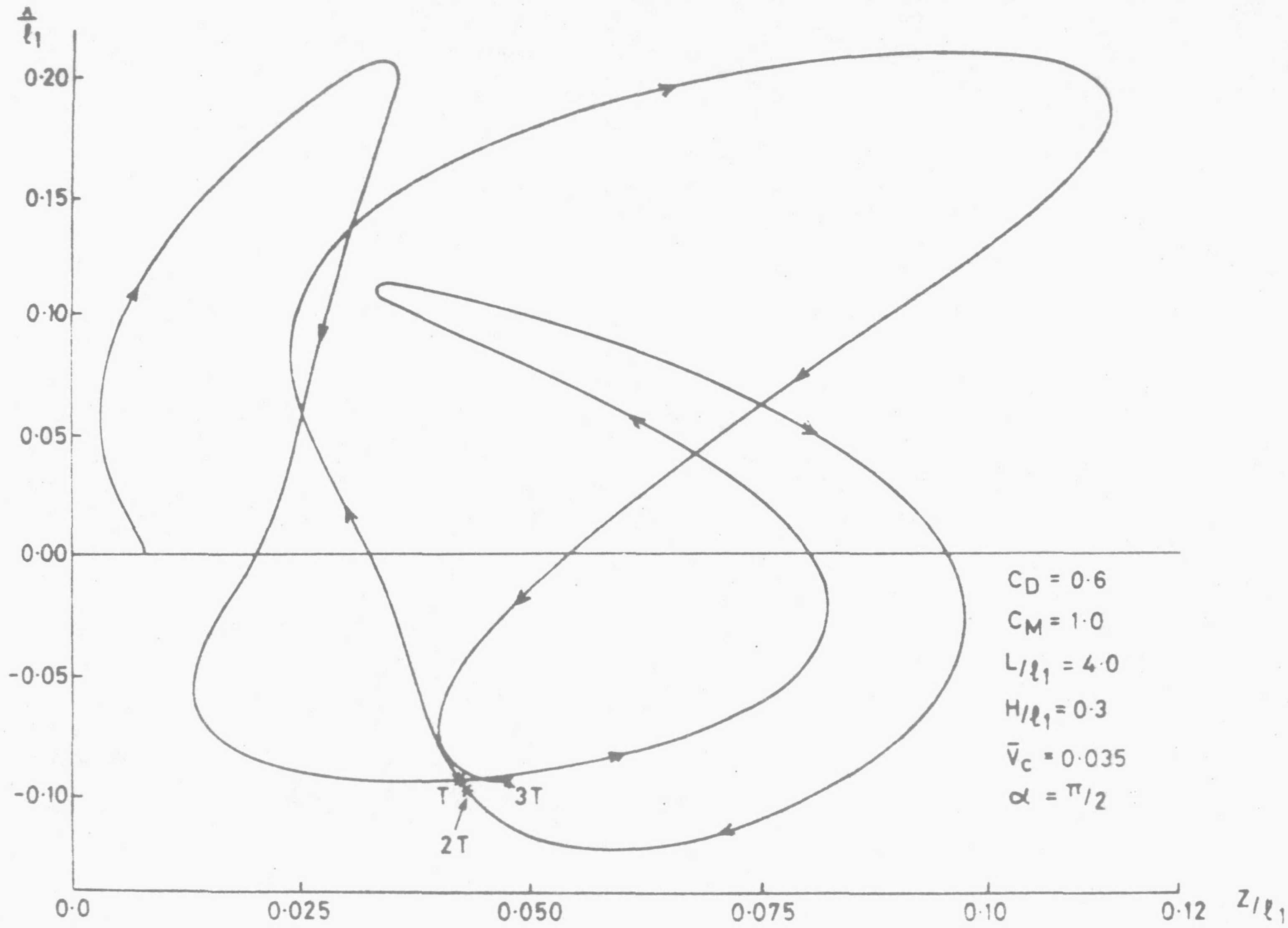

Fig. 7a

Response to orthogonal Waves and Current - Point O_2

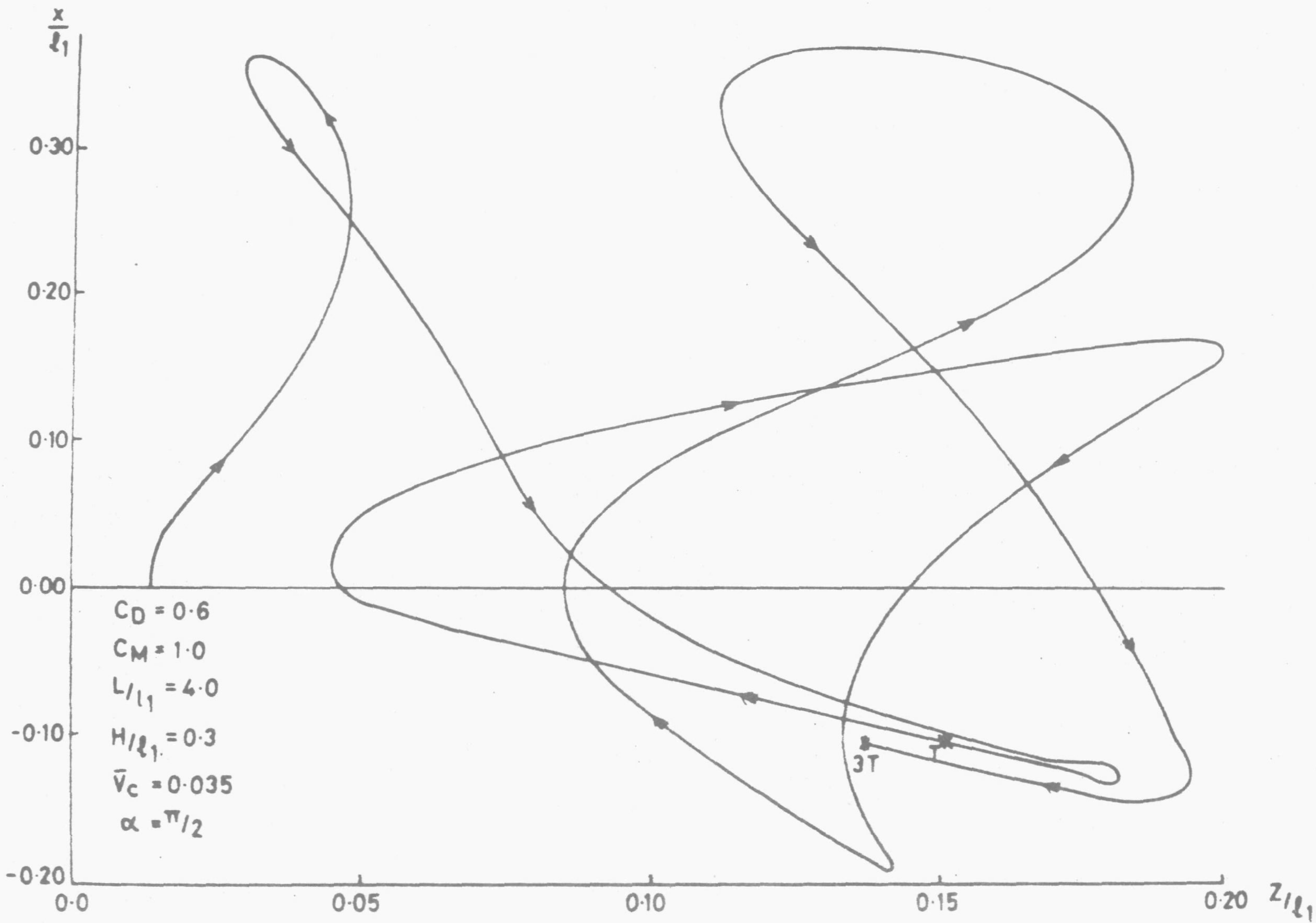

Fig. 7b

Response to orthogonal waves and current - Top

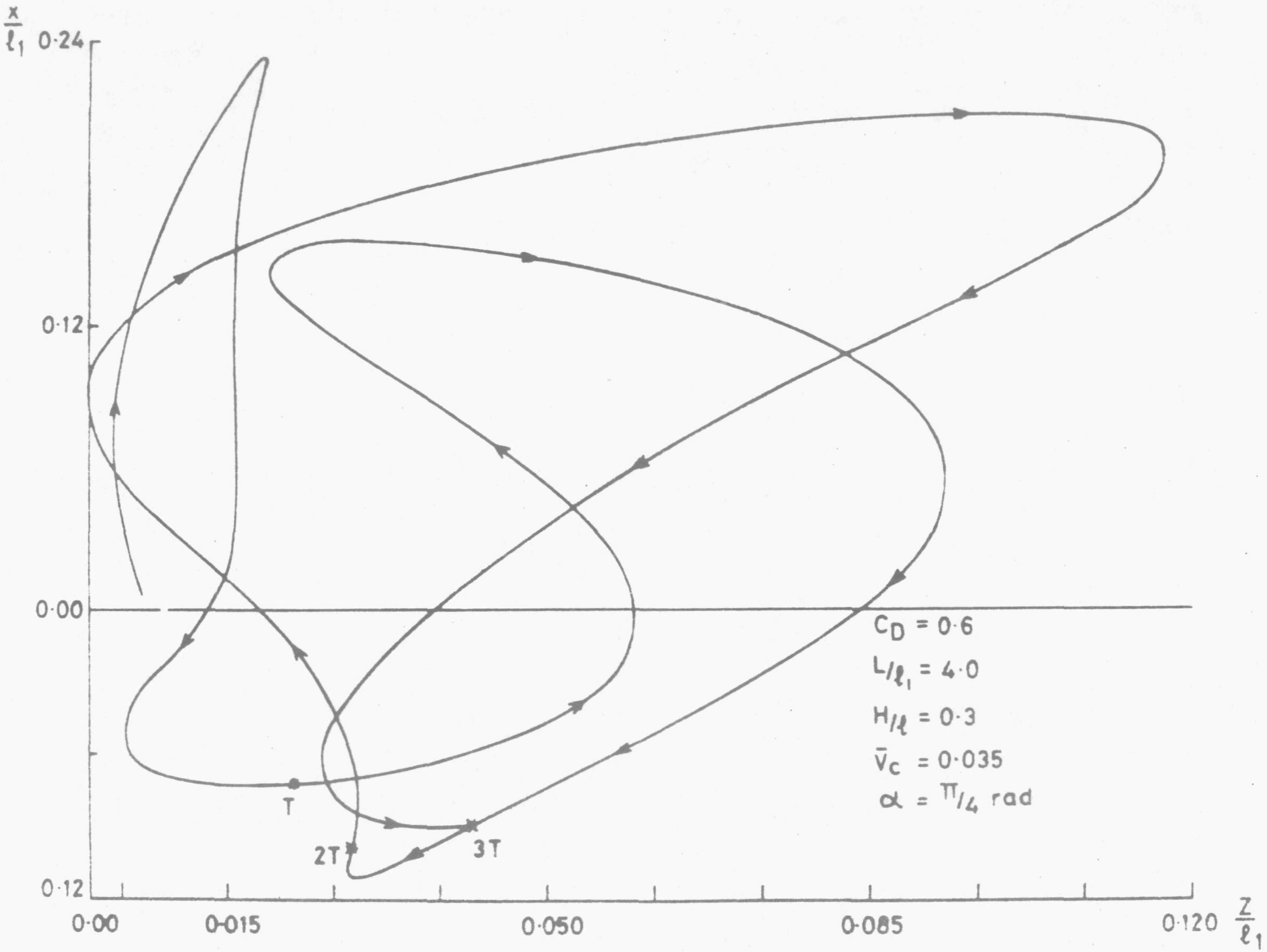

Fig. 8a

Response to waves and current at an angle $\alpha = \pi/4$ - Point O_2

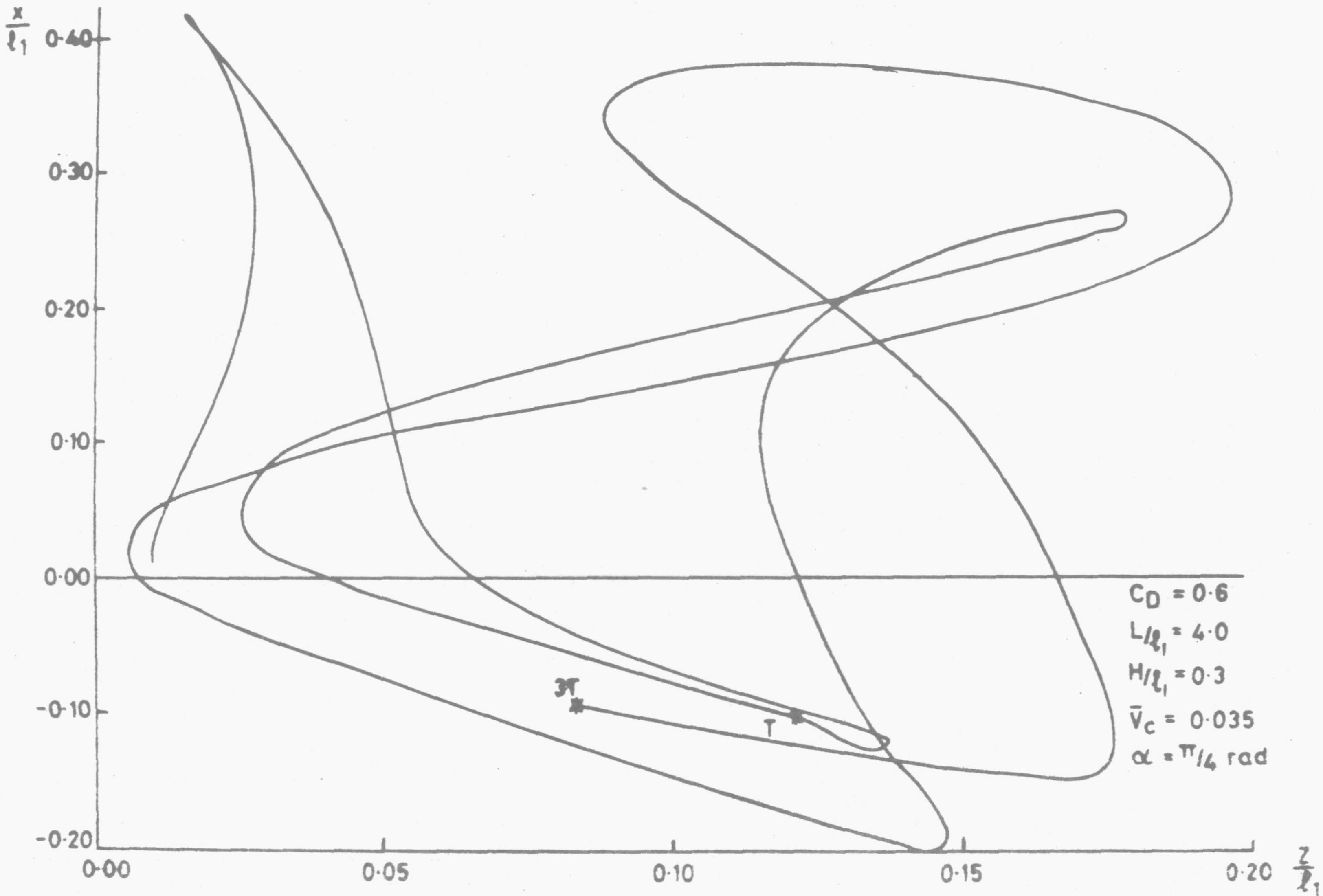

Fig. 8b

Response to waves and current at an angle $\alpha = \pi/4$ - Top